# Kinetic and Spectroscopic Studies of the Molybdenum-Copper CO Dehydrogenase from *Oligotropha carboxidovorans*\*

**Bo Zhang, Craig F. Hemann, and Russ Hille**[1]

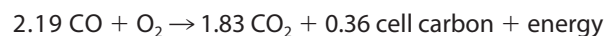*From the Department of Biochemistry, University of California, Riverside, California 92521*

Carbon monoxide dehydrogenase from the aerobic bacterium *Oligotropha carboxidovorans* catalyzes the oxidation of CO to $CO_2$, yielding two electrons and two $H^+$. The steady-state kinetics of the enzyme exhibit a pH optimum of 7.2 with a $k_{cat}$ of 93.3 $s^{-1}$ and $K_m$ of 10.7 $\mu M$ at 25 °C. $k_{red}$ for the reductive half-reaction agrees well with $k_{cat}$ and exhibits a similar pH optimum, indicating that the rate-limiting step of overall turnover is likely in the reductive half-reaction. No dependence on CO concentration was observed in the rapid reaction kinetics, however, suggesting that CO initially binds rapidly to the enzyme, possibly at the Cu(I) of the active site, prior to undergoing oxidation. A Mo(V) species that exhibits strong coupling to the copper of the active center ($I = 3/2$) has been characterized by EPR. The signal is further split when [$^{13}$C]CO is used to generate it, demonstrating that substrate (or product) is a component of the signal-giving species. Finally, resonance Raman spectra of CODH reveal the presence of FAD, Fe/S clusters, and a [$CuSMoO_2$] coordination in the active site, consistent with earlier x-ray absorption and crystallographic results.

*Oligotropha carboxidovorans* is a carboxydotrophic bacterium capable of aerobic, chemolithoautotrophic growth using CO as a sole source of carbon and energy (1, 2). The key enzyme involved in this facultative metabolism is an air-stable molybdenum-containing CO dehydrogenase (CODH)[2] that catalyzes the oxidation of CO to $CO_2$ according to Equations 1 and 2,

$$CO + H_2O \rightarrow CO_2 + 2H^+ + 2e^-$$

(Eq. 1)
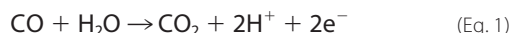
$$\Delta E^\theta = -558 \text{ mV}$$

(Eq. 2)

at pH 7. The reducing equivalents obtained from CO are transferred through an electron transfer chain to reduce molecular oxygen. $CO_2$ thus generated is fixed non-photosynthetically via the pentose phosphate cycle (3, 4) with the following overall reaction stoichiometry in Equation 3.

[2] The abbreviations used are: CODH, carbon monoxide dehydrogenase; XOR, xanthine oxidoreductase; ICP-AES, inductively coupled plasma atomic emission spectrometer; EPR, electron paramagnetic resonance; rR, resonance Raman; CAPS, 3-(cyclohexylamino)propanesulfonic acid; MES, 4-morpholineethanesulfonic acid; CHES, 2-(cyclohexylamino)ethanesulfonic acid.

$$2.19 \text{ CO} + O_2 \rightarrow 1.83 \text{ } CO_2 + 0.36 \text{ cell carbon} + \text{energy}$$

(Eq. 3)

This molybdenum-containing CODH is distinct from the highly $O_2$-sensitive, Ni/Fe-containing CODH from obligate anaerobes such as *Clostridum thermoaceticum* or *Methanosarcina barkerii* (5). The Mo-containing CODH from *O. carboxidovorans* and *Hydrogenophaga pseudoflava* have been structurally characterized (6–10). Both are $(\alpha\beta\gamma)_2$ hexamers consisting of a small subunit (CoxS, 17.8 kDa) that has two [2Fe-2S] clusters, a medium subunit (CoxM, 30.2 kDa) that possesses FAD, and a large subunit (CoxL, 88.7 kDa) that has the active site molybdenum center (11, 12).

The Mo-containing CODH exhibits significant structural and sequence homologies to xanthine oxidoreductase (XOR) and other molybdenum hydroxylases (13). Given the nature of the reaction catalyzed, however, CODH is of interest to gain a better understanding of the general activity of such molybdenum centers in biology. CODH is also of significant environmental interest as it is involved in the clearance of CO from the environment. Aerobic organisms such as *O. carboxidovorans* have been estimated to remove $\sim 2 \times 10^8$ metric tons of CO from the atmosphere annually (14).

Despite some initial confusion about the structure of the active site of CODH, the metal center has recently been established by high resolution x-ray crystallography (6, 7) and x-ray absorption spectroscopy (15) to be a binuclear [$Cu^I SMo^{VI}$] cluster, with the two metal atoms bridged by a $\mu$-sulfido ligand. A reaction mechanism has been proposed involving the formation of an $SCO_2$ intermediate, on the basis of the crystal structure of CODH in complex with the inhibitor *n*-butylisocyanide (7). However, computational studies suggest that such a thiocarbonate intermediate actually leads to a deep minimum on the potential energy surface, making $CO_2$ release extremely difficult (16, 17). In addition, model compound studies suggest that CO oxidation could occur directly at the Cu(I) site, followed by electron transfer to Mo via the electronic delocalization of the Mo($\mu$-S)Cu moiety (18). Here, we report a study of the kinetic and spectroscopic properties of CODH to gain better insight into the nature of the active site and the mechanism by which CO is oxidized.

## EXPERIMENTAL PROCEDURES

*Materials*—Carbon monoxide gas was obtained from Airgas at a purity of 99.5%. Isotopically enriched $^{98}MoO_3$ ($^{98}$Mo, 99%), $^{13}$CO ($^{13}$C, 99%), and $D_2O$ ($^2$H, 99.9%) were from Cambridge

Isotope Lab, Inc. All other chemicals and reagents were obtained at the highest quality/purity available commercially and were used without further purification.

*Bacteria Growth and Enzyme Purification*—*O. carboxydovorans* (ATCC 49405) was cultivated at 30 °C, pH 7 in a 20-liter fermentor (BioFlo 415, New Brunswick) containing carboxydobacterium medium (9), with a gas mixture of 50% CO and 50% air. Cells were harvested in the late exponential phase ($A_{436}$ >5), washed in 50 mM HEPES (pH 7.2), and stored at −80 °C. $^{98}$Mo-enriched CODH was obtained from *O. carboxydovorans* grown in $^{98}$MoO$_3$-substituted medium.

CODH was purified using the procedure described by Meyer *et al.* (9, 19) with some modifications. All chromatography steps were carried out on an ÄKTA purifier (GE Healthcare) at 4 °C. About 60 g of thawed cells were suspended in 100 ml of 50 mM HEPES, pH 7.2 containing 1 mM EDTA, 0.2 mM phenylmethylsulfonyl fluoride, and 5 mg of DNase I, and disrupted with a French press (FA-078A, Thermo Electron Co.). Cell debris was removed by ultracentrifugation at $100,000 \times g$ for 2 h. The supernatant was loaded onto a Q-Sepharose column (40 cm × 2.6 cm) pre-equilibrated with 50 mM HEPES, pH 7.2, and eluted with seven column volumes of a linear gradient of 0–0.8 M NaCl in 50 mM HEPES, pH 7.2. Fractions possessing CODH activity (see below) were pooled, concentrated in an Amicon concentrator with 100-kDa MW cut-off, and passed through a Sephacryl S-300 column (40 cm × 2.6 cm) equilibrated (and eluted) with 50 mM HEPES, pH 7.2. Fractions were analyzed for both CODH activity and optical spectra, and only those of high activity and spectral purity (as judged by the absence of heme contaminants absorbing at 420 nm) were pooled and concentrated. Purified enzyme had an absorbance ratio of $A_{280}/A_{450}$ ~5.5 and $A_{450}/A_{550}$ ~2.9, and exhibited only three bands by SDS-polyacrylamide gel electrophoresis (7.5% stacking gel and 12% resolving gel) and a single band by non-denaturing PAGE (5% stacking gel and 7.5% resolving gel). The purified enzyme was stored in liquid nitrogen until needed.

*Protein Estimation and Enzyme Assay*—Protein concentrations were determined by the Bradford method (20). The extinction coefficient of purified enzyme at 450 nm was determined to be 70 mM$^{-1}$ cm$^{-1}$ for the $(\alpha\beta\gamma)_2$ hexamer, very close to the reported value of 72 mM$^{-1}$ cm$^{-1}$ (21, 22), which was used to calculate the concentration of enzyme.

CODH activity was monitored spectrophotometrically by the CO-dependent reduction of methylene blue ($\epsilon_{615} = 37.11$ mM$^{-1}$ cm$^{-1}$) at 30 °C (23). A rubber septum-stoppered cuvette containing 50 $\mu$M methylene blue in 2 ml of 50 mM potassium phosphate, pH 7.2 was bubbled with 100% CO for 10 min, and then 10 to 20 $\mu$l of anaerobic enzyme was injected via Hamilton syringe to initiate the reaction. The absorbance change was monitored at 615 nm using a UV-visible spectrophotometer (HP 8452A). With one unit of activity defined as 1 $\mu$mol of CO oxidized per min at 30 °C, pure CODH exhibited a specific activity of 11.3 units/mg with methylene blue as the electron acceptor. Fully functional enzyme was earlier reported to have a specific activity of ~24 units/mg using 1-phenyl-2-(4-iodophenyl)-3-(4-nitrophenyl)-2*H*-tetrazolium chloride (INT) and 1-methoxyphenazine methosulfate (MPMS) as the electron acceptors (7). In our hands, the INT/MPMS assay was >1.5

times faster than that with methylene blue under the same conditions, indicating that our enzyme preparation had comparable activity to that seen previously.

Fe, Mo, Cu, and Se contents were determined by inductively coupled plasma atomic emission spectrometry (ICP-AES, Optima 3000 DV, Perkin Elmer). Analysis of the results revealed 8.05 Fe, 1.82 Mo, and 1.69 Cu per mol of enzyme dimer. Mo and Cu are both essential for CODH activity (15, 22), and these results suggest that ~15% of our CODH preparation is nonfunctional because of incomplete metal incorporation into apoprotein.

*Reductive Titration with Sodium Dithionite*—Reductive titrations of CODH were carried out in 50 mM potassium phosphate, pH 7.2 or 50 mM CAPS, 0.1 N NaCl, pH 10 at room temperature (22 °C). Enzyme, typically at a concentration of ~10 $\mu$M, was made anaerobic in a sealed cuvette by repeated vacuum-flushing with argon. Sodium dithionite was dissolved in anaerobic buffer and titrated into the enzyme solution via a gas-tight syringe. The concentration of sodium dithionite in the stock solution was determined from the absorbance at 314 nm ($\epsilon = 8.0$ mM$^{-1}$ cm$^{-1}$; Ref. 24).

*Steady-state Kinetics*—Steady-state kinetics was carried out under anaerobic conditions in 50 mM potassium phosphate, pH 7.2 at 25 °C using a stopped-flow spectrophotometer (Applied Photophysics). One syringe was loaded with anaerobic CODH (4.4 nM, after mixing), and the other with CO-flushed methylene blue (36 $\mu$M) in KH$_2$PO$_4$ buffer. The concentrations of CO were calculated based on a solubility of 1.0 mM at 1 atm and 25 °C (25). CO concentrations of 10–438 $\mu$M were obtained by mixing CO-flushed methylene blue with argon-flushed methylene blue. Absorbance changes were monitored at 615 nm, and the initial rates were plotted against CO concentration to obtain $k_{cat}$ and $K_m$.

*Rapid Reaction Kinetics*—The reductive half-reaction of CODH (i.e., the reaction of $E_{ox}$ with CO under anaerobic conditions) was carried out by stopped-flow at 4 °C, over the pH range 5.5–10. Enzyme concentrations of 6–10 $\mu$M were mixed with various concentrations of CO, and the spectral change recorded over an appropriate period of time. The activation energy of CODH reduction by CO was determined at pH 7.2 and pH 10 from the temperature dependence of the reaction of enzyme with 1.0 mM CO over the temperature range 4 to 30 °C. The fast phases of the kinetic traces (see below) were fit to single exponentials using Pro-Kineticist software to obtain the observed rate constant ($k_{obs}$).

*Electron Paramagnetic Resonance and Resonance Raman Spectroscopy*—EPR spectra were recorded using a Brüker Instruments ER 300 spectrometer equipped with an ER 035 M gaussmeter and a HP 5352B microwave frequency counter. Temperature was controlled at 150 K using a Brüker ER 4111VT liquid N$_2$ cryostat. In experiments with substoichiometric CO, 200 $\mu$l of 50 $\mu$M anaerobic CODH in 50 mM potassium phosphate, pH 7.2 were added to a sealed EPR tube filled with argon. 10 $\mu$l of CO-flushed buffer (containing ~23 $\mu$M CO) were then added and mixed by micropipetting. The solution was incubated for 10 s, then frozen in an acetone/liquid nitrogen bath. Other samples were prepared by reacting CODH
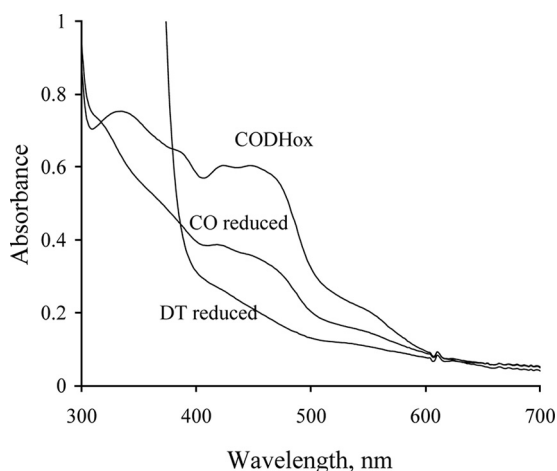
FIGURE 1. **UV-vis absorption spectra of CODH.** Spectra are for the oxidized form, CO-reduced form (1 min after mixing), and sodium dithionite-reduced form. The spectra were recorded in 50 mM HEPES, pH 7.2.
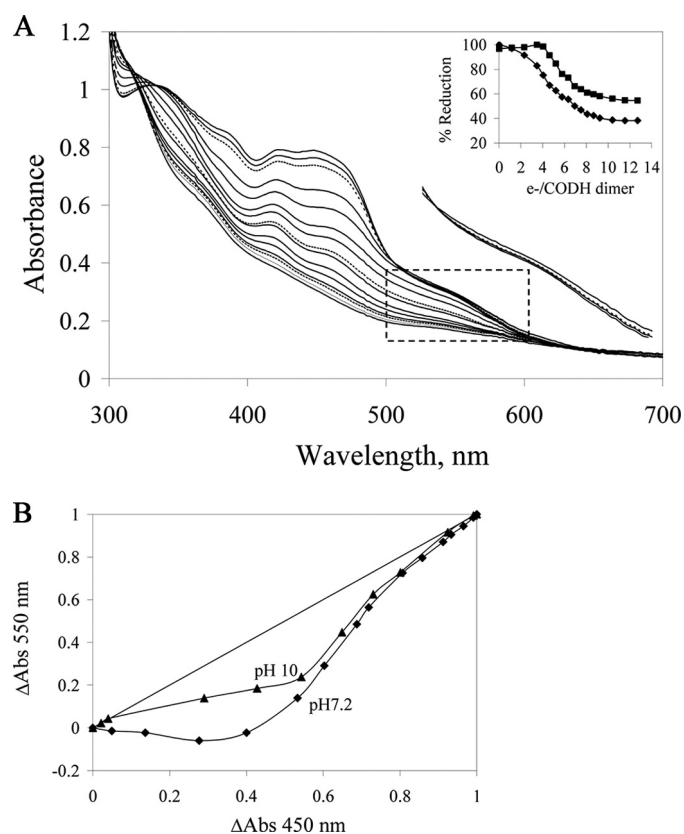


FIGURE 2. **Reductive titration of CODH with sodium dithionite under anaerobic conditions.** *A*, spectral changes seen on titration of CODH with sodium dithionite in 50 mM potassium phosphate, pH 7.2. To the *right* of the main set of spectra is an enlargement of the *boxed area* for three spectra early in the titration, demonstrating a transient absorption increase with the earliest additions of reductant. The *lowermost spectrum* is that of oxidized enzyme, the *dashed spectrum* the enzyme after addition of the first aliquot of dithionite, and the *uppermost spectrum* that seen after addition of the second aliquot. *Inset*, absorbance changes at 450 nm (*diamonds*) and 550 nm (*squares*) *versus* reducing equivalents added per CODH dimer. *B*, plots of relative absorbance changes at 550 nm *versus* 450 nm at pH 7.2 (*diamonds*) and pH 10 (*triangles*).

with excess reductant (CO or sodium dithionite). A frozen water sample was used for background correction.

The EPR spectrum of reduced CODH in $D_2O$ was obtained by exchanging CODH into Tris-$D_2O$ buffer (50 mM, pD 7.6) by passage of enzyme through a Sephadex G-25 column equilibrated with that buffer, followed by reaction with excess CO. The EPR spectrum of enzyme reduced with $^{13}CO$ was obtained simply by reaction with $^{13}C$-labeled CO (99%, Cambridge Isotope Lab) in 50 mM Tris, pH 8.0. Simulation of the EPR spectrum of CO-reduced $^{98}Mo$-labeled CODH was performed using EasySpin, a free software developed by Stefan Stoll at University of California, Davis.

Resonance Raman spectra were obtained using 514.5 nm excitation from a Coherent Innova 307 argon ion laser. Raman-scattered light was collected and dispersed using a single-stage spectrograph into a Princeton Instruments 1024 KTB, back-thinned, charge-coupled device detector. Calibration was performed using an external indene standard with reported band positions accurate to $\pm 2$ cm$^{-1}$. Data were collected from the surface of a 30-$\mu$l sample ($\sim$250 $\mu$M, in 50 mM HEPES buffer, pH 7.2) held at 30 K in a custom-built cold finger with a APD Cryogenics closed-cycle helium refrigerator. Samples were illuminated at 30 K for several hours prior to data collection to reduce background fluorescence. This procedure did not demonstrably change the resonance Raman line positions, but simply reduced the background.

## RESULTS

*Determination of the Extent of Functional CODH*—To assess the catalytic competence of the CODH used here, the extent of reduction of the enzyme by CO under anaerobic conditions was compared with that by dithionite (7). As shown in Fig. 1, exposure to CO for 1 min reduced the absorbance at 450 nm by $\sim$62% in comparison to the dithionite-reduced enzyme, depending on the preparation. Further incubation of the enzyme with CO ($\sim$30 min) resulted in complete reduction, similar to the dithionite-reduced form. Such behavior has been observed with other Mo-containing enzymes, notably xanthine oxidoreductase (13), and has been ascribed to the presence of a

certain amount of non-functional enzyme that becomes reduced by slow intermolecular electron transfer from the reduced functional enzyme (which subsequently reacts with more substrate to become fully reduced once again). In all experiments described here, the concentration of functional enzyme was used, correcting the total enzyme concentration for the amount of non-functional enzyme determined as described above.

*Titration of CODH with Sodium Dithionite*—Fig. 2 shows reductive titrations of CODH with sodium dithionite as performed at pH 7.2 and pH 10. In total, approximately twelve reducing equivalents per CODH dimer were required to reach the end point (Fig. 2A, *inset*), consistent with the constitution of the protein redox-active centers. At pH 7.2, the first four reducing equivalents resulted in a significant decrease in absorbance at 450 nm and a slight increase above 550 nm, suggesting accumulation of the neutral FADH$^\bullet$ semiquinone. Further titration resulted in a decrease in absorbance at both 450 nm and 550 nm, consistent with reduction of FADH$^\bullet$ on to FADH$_2$ along with additional reduction of the Fe/S clusters.

The relative reduction potentials of FAD and Fe/S centers were gauged by plotting the fractional absorbance changes at
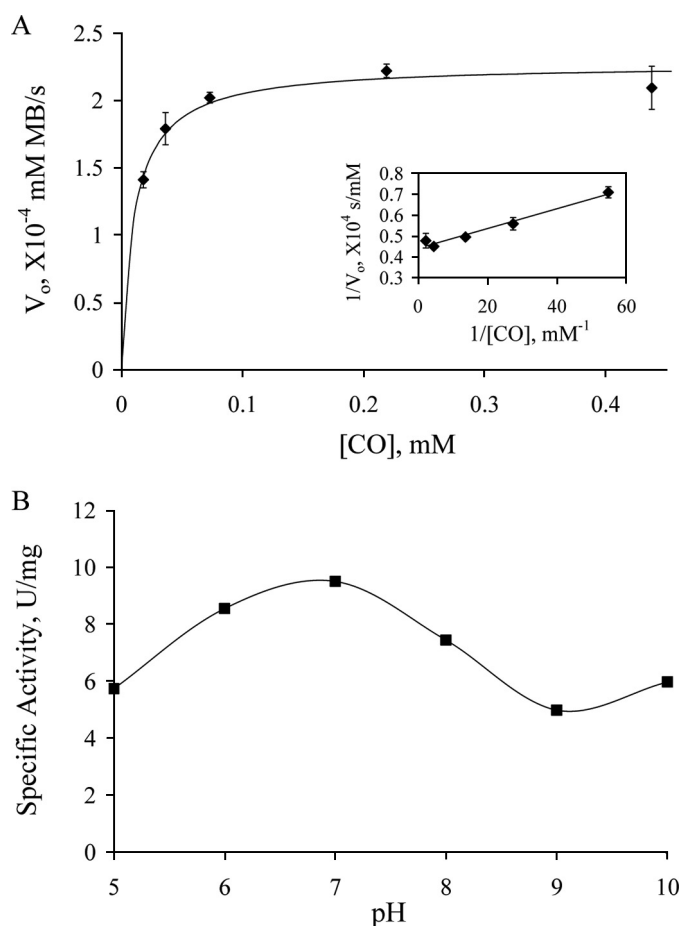
FIGURE 3. **Steady-state kinetics of CODH reaction with CO using methylene blue as the electron acceptor.** *A*, plot of initial rate (following the absorbance decrease at 615 nm upon reduction of methylene blue, after mixing 4.4 nM CODH with CO-dissolved (10–438 $\mu$M) methylene blue) as a function of [CO] in 50 mM potassium phosphate, pH 7.2, 25 °C. The *solid line* is the fit with the Michaelis-Menten equation using kinetic parameters obtained from the double-reciprocal plot (*inset*). *B*, the pH dependence of CODH activity, with specific activity given in units/mg, and 1 unit is 1 $\mu$mol of CO oxidized/min. Buffers used in the experiments are: MES pH 5.5, potassium phosphate pH 6 and 7, Tris pH 8, CHES pH 9, and CAPS pH 10, all at 50 mM.

450 nm (where the FAD and Fe/S centers contribute approximately equally to the absorbance change observed upon reduction of the enzyme) *versus* 550 nm (where the Fe/S centers are responsible for the entirety of the spectral change) (26, 27). Fig. 2*B* shows plots of the fractional absorbance change at 550 nm *versus* that at 450 nm seen in reductive titrations at pH 7.2 and pH 10. The data at pH 7.2 resemble those seen previously with XOR (27). On the other hand, the pH 10 data continue to trend toward the lower right in the plot, whereas with XOR at pH 10 the plot trends strongly to the upper left (27). These results indicate that, particularly at high pH, the midpoint potential of FAD is substantially higher relative to the average of the potentials for the two Fe/S clusters in CODH (we estimate by at least 30 mV), whereas the reverse is true with XOR.

*Steady-state Kinetics*—Fig. 3*A* shows the [CO] dependence of turnover at 25 °C using methylene blue as the electron acceptor. The data yield a $k_{cat}$ of 57.8 s$^{-1}$ and $K_m$ of 10.7 $\mu$M, with a $k_{cat}/K_m$ of $8.7 \times 10^6$ M$^{-1}$ s$^{-1}$. As shown in Fig. 1*C*, the enzyme used in the assay was ~62% active (as judged by the functionality test described above), and the corrected turnover number

for the fully functional enzyme is thus 93.3 s$^{-1}$. This compares favorably with the value of 107 s$^{-1}$ at 30 °C seen with INT as the electron acceptor (7), particularly when the 5 °C difference in temperature is taken into account.

CODH has a pH optimum of ~7.2 (Fig. 3*B*), the pH at which most of the experiments here were carried out. It is noteworthy, however, that even at extremes in pH where the enzyme is only marginally stable CODH retains more than half of its maximal activity (Fig. 3*B*). The only modest loss of activity at these extreme pHs indicates that ionization of functional groups in the active site is not as critical to catalysis for CODH as has been found for XOR (30).

*Reductive Half-reaction of CODH with CO*—The rapid reaction kinetics of CODH with CO were determined at pH 7.2, 4 °C using stopped-flow spectrophotometry. Enzyme reduction was followed via the spectral change associated with reduction of the (functional) enzyme. Fig. 4*A* shows the time course seen for the absorption change at 450 nm. The reaction is distinctly biphasic, with a fast phase occurring in the first 500 ms, followed by a much slower reaction on a hundreds of seconds time scale (Fig. 4*A*, *inset*). By analogy to the kinetic behavior seen with XOR (31), the initial fast phase of the reaction is attributed to the reduction of the functional portion of the enzyme, after which a slow intermolecular transfer of reducing equivalents to the nonfunctional portion of the enzyme occurs (with subsequent re-reduction of the functional enzyme). The relative amplitudes of the fast and slow phases suggest that the enzyme used was ~65% functional, in good agreement with the above spectrophotometric results. Surprisingly, at all pH values examined, no [CO] dependence of $k_{obs}$ for the fast phase of the reaction (hereafter referred to as $k_{red}$) is observed over the concentration range 30 to 476 $\mu$M (Fig. 4*A*). At pH 7.2 and 4 °C, $k_{red}$ is determined to be 11.4 s$^{-1}$. The rate constant for the slower phase of the reaction is found to be modestly pH-dependent. At higher pH the intermolecular electron transfer becomes somewhat faster ($k_{slow}^{app}$ = 0.046 and 0.070 s$^{-1}$ at pH 7 and 9, respectively).

Because $k_{red}$ exhibited no dependence on [CO], no $K_d$ could be determined. This kinetic behavior resembles that seen with XOR and slow substrates, and is consistent with the initial rapid formation of a Cu$^I$·CO complex prior to oxidation of substrate, as has been suggested in the literature (16–18). The pH dependence of $k_{red}$ exhibits a maximum at pH 7.2 (Fig. 4*C*), in agreement with the above steady-state results and suggesting that the rate-limiting step of turnover is in the reductive half-reaction.

The temperature dependence of $k_{red}$ was investigated at pH 7.2 and pH 10 under CO-saturating conditions. Table 1 lists the activation parameters calculated from both an Arrhenius (Fig. 5*A*) and an Eyring (Fig. 5*B*) analysis of the data. The activation energy for the reaction of CODH with CO is 47.8 kJ/mol at pH 7.2 and 43.1 kJ/mol at pH 10.

At 25 °C and pH 7.2, $k_{red}$ is 51.1 s$^{-1}$, some 4-fold faster than at 4 °C. This value is approximately half the observed $k_{cat}$ of 93.3 s$^{-1}$ from steady-state kinetics at the same temperature (after correction for nonfunctional enzyme). This disparity has been accounted for previously by Olson *et al.* (26) in the case of XOR, and is due to the fact that under the present reaction conditions
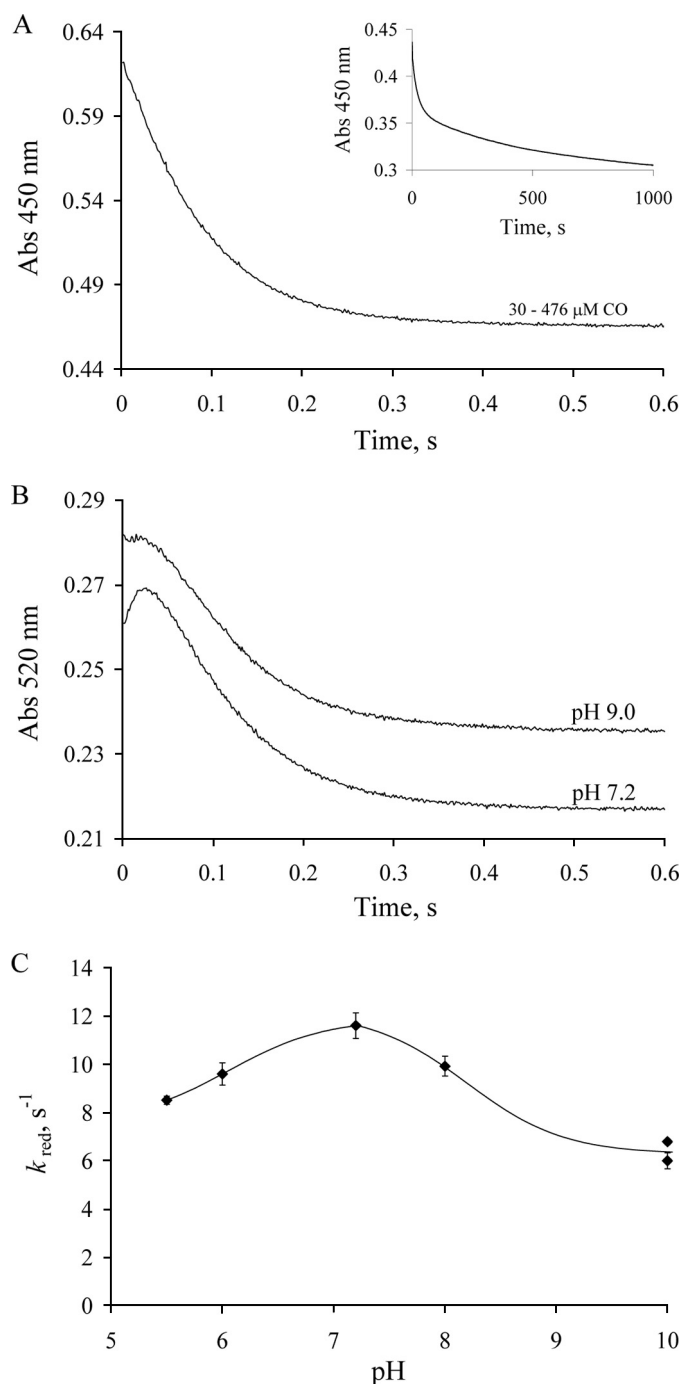
A



B



C



FIGURE 4. **Kinetics of CODH reduction by excess CO under anaerobic conditions.** *A*, the kinetic trace seen at 450 nm upon mixing 12 $\mu$M CODH with 30–476 $\mu$M CO in 50 mM potassium phosphate, pH 7.2, 4 °C (transients at different CO concentrations are overlapping). *Inset*, the absorbance change over 1000 s. *B*, the kinetic traces at 520 nm at pH 7.2 and pH 9 (50 mM CHES). Curves at different CO concentrations (30–476 $\mu$M) are overlapping. *C*, the pH dependence of $k_{red}$ for CODH reduction at 4 °C.

three successive substrate molecules must react with enzyme to achieve complete reduction. The observed $k_{red}$ has been shown to underestimate the actual rate constant for an individual step by a factor of two. Taking this into consideration, $k_{red}$ as determined from the rapid reaction kinetics (51 s$^{-1}$) agrees well with the steady-state $k_{cat}$ (93 s$^{-1}$). In conjunction with the similar pH dependence seen for the steady-state and reductive half-reac-

TABLE 1
**Activation parameters of CODH reduction by CO at pH 7.2 and pH 10**
The conditions are the same as in Fig. 5.

|  | pH 7.2 | pH 10 |
|---|---|---|
| $E_a$, kJ/mol | 47.8 | 43.1 |
| $\Delta H^{\ddagger}$, kJ/mol | 45.4 | 40.7 |
| $\Delta S^{\ddagger}$, J/K·mol | −60.4 | −83.9 |
| $\Delta G$, kJ/mol | 63.4 | 65.7 |

A



B
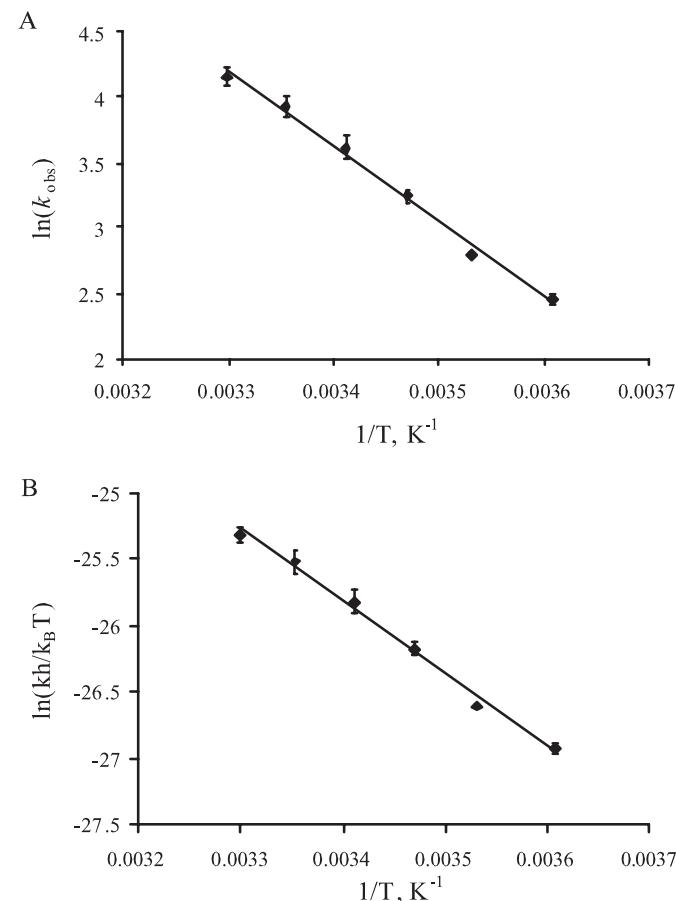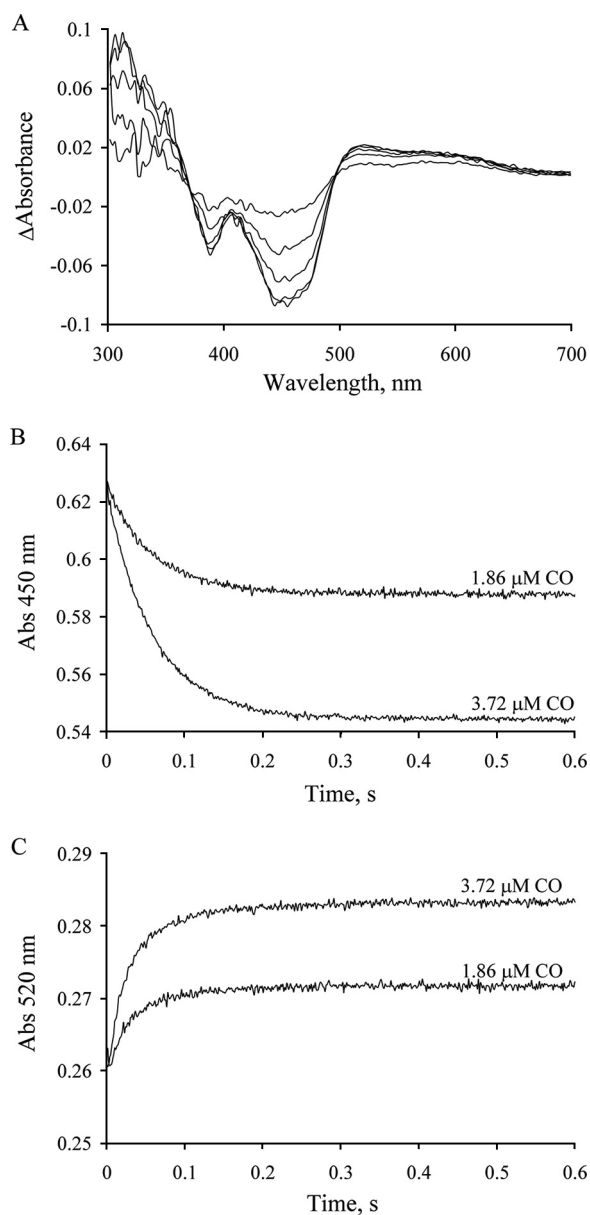


FIGURE 5. **The effect of temperature on the reduction of CODH by CO.** Observed rate constants were determined at 4–30 °C after mixing 10 $\mu$M CODH with CO-saturated potassium phosphate, pH 7.2. An Arrhenius plot (*A*) or Erying's plot (*B*) was used to determine the activation energy of CODH reduction.

tion kinetics, this indicates that the latter is principally rate-limiting in CODH catalysis.
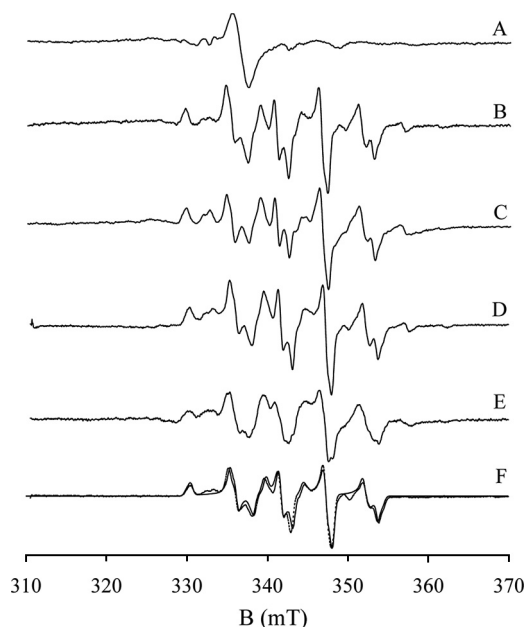
At pH 7.2 and 4 °C, the kinetic transients at 520 nm exhibit a small initial increase followed by a subsequent decrease (Fig. 4*B*, *lower curve*). The amplitude of the first phase is very small, with an apparent rate constant estimated to be 65 s$^{-1}$. For the second phase $k_{obs}$ is 10.2 s$^{-1}$, in good agreement with the value of 11.4 s$^{-1}$ seen at 450 nm. The transient absorbance increase is pH-dependent. At pH 5.5 the initial increase becomes more pronounced; but at pH 9 or 10, only a lag phase is observed, with no transient absorbance increase (Fig. 4*B*, *upper curve*). In combination with the reductive titration data discussed above, we conclude that the transient absorption increase is due to FADH$^{\cdot}$ accumulating in partially reduced enzyme forms (CODH$_{2e-}$, CODH$_{4e-}$) generated early in the course of the reaction with CO.

FIGURE 7. **EPR spectra of reduced CODH.** Samples were prepared as follows (all in 50 mM potassium phosphate, pH/D 7.2): *A*, 50 μM CODH reduced with 23 μM CO for 10 s at 4 °C. The peak-to-trough line width of the isotropic radical signal is 20 Gauss. *B*, CODH reduced with excess CO under the same buffer conditions; *C*, CODH reduced sodium dithionite; *D*, CODH reduced with CO in Tris-D$_2$O buffer, pH 8; *E*, CODH reduced with $^{13}$CO; *F*, $^{98}$Mo-enriched CODH reduced with CO (*solid line*), and simulation of the spectrum (*dashed line*) with parameters g$_{1,2,3}$ = 2.0010, 1.9604, 1.9549, A$_{1,2,3}$ = 117, 164, 132 MHz, $\alpha$ = 0, $\beta$ = 40, $\gamma$ = 40. The EPR instrument settings were: 9.455 GHz microwave frequency; 10 milliwatt microwave power; 5 Gauss modulation amplitude; 150 K.

increases ($k_{obs}$ = 29.5 s$^{-1}$) and does not subsequently decrease as is seen in the reaction with excess CO, again reflecting significant accumulation of FADH$^{\bullet}$ in the reaction.

*EPR and Resonance Raman Studies of CODH*—To confirm that the neutral FADH$^{\bullet}$ semiquinone is indeed formed to a significant degree upon partial reduction of the enzyme, we examined the enzyme by EPR spectroscopy. The spectrum of CODH reduced with limiting CO yields an isotropic radical signal centered at g ~2.003 with a peak-to-trough line width of 20 G (Fig. 7*A*), indicative of the neutral flavin semiquinone. The integrated spin intensity of this isotropic signal, calibrated using a Cu-EDTA standard, accounted for ~20% of FADH$^{\bullet}$ accumulation.

Functional CODH is EPR silent in the air-oxidized state, implying that the copper ion in the active site is present as Cu(I). Inactive CODH, by contrast, shows a small resting Mo(V) signal resembling the "Resting I" and "Inhibited" signals seen with XOR (22, 32) that is presumably because of enzyme that has lost the catalytically essential copper and bridging sulfur. In our hands, the EPR spectra of CO- or dithionite-reduced CODH (Fig. 7, *B* and *C*) were essentially identical, but differed in detail to previously published spectra (the latter appearing to arise from more than one paramagnetic species; Ref. 22). Our spectrum has well-resolved structure suggestive of hyperfine interactions with both Mo and Cu nuclei. The small satellite features attributable to the combined 25% natural abundance of $^{95}$Mo and $^{97}$Mo (18), at 3275, 3575, and 3625 G, are lost in $^{98}$Mo-labeled enzyme (Fig. 7 F, *solid line*). The quartet features arising from the I = 3/2 nuclei of $^{63,65}$Cu are readily evident in







FIGURE 6. **Kinetics of reduction of CODH with substoichiometric CO under anaerobic conditions.** *A*, difference spectra seen in the course of the reaction of 12 μM CODH with 3.72 μM CO (at 0.02, 0.05, 0.1, 0.2, and 1 s after mixing) in 50 mM potassium phosphate, pH 7.2, 4 °C. All absorbance changes are given relative to the oxidized enzyme. *B* and *C*, kinetic transients observed at 450 nm and 520 nm, respectively, upon mixing 12 μM CODH with 3.72 or 1.86 μM CO in 50 mM potassium phosphate, pH 7.2, 4 °C.

*Reduction of CODH with Substoichiometric CO*—Reaction of enzyme with substoichiometric concentrations of substrate has proven useful in simplifying the observed kinetics of other systems, because under these conditions no enzyme molecule is likely to react with more than one equivalent of substrate (29). Fig. 6*A* shows the difference spectra (relative to oxidized enzyme) seen in the course of the reaction of 12.5 μM CODH with either 1.86 or 3.72 μM CO in 50 mM potassium phosphate, pH 7.2. They exhibit well-maintained isosbestic points at 370 and 496 nm. The absorbance at 450 nm decreases monotonically and in proportion to the substrate concentration (Fig. 6*B*). The observed rate constant is 16.7 s$^{-1}$, slightly greater than that with excess CO. Above 520 nm the absorbance
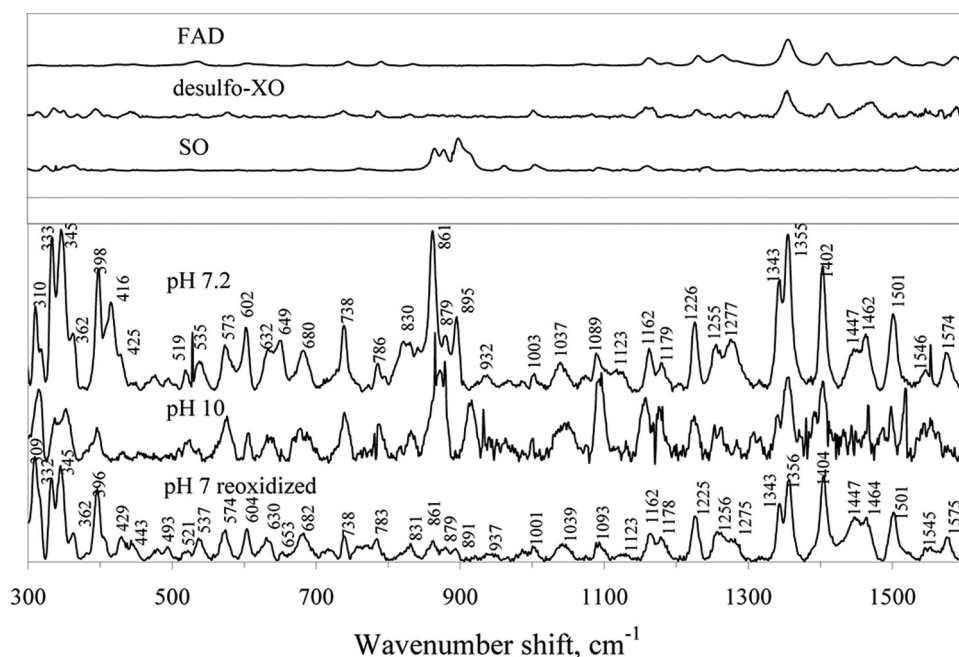
FIGURE 8. **Resonance Raman spectra of oxidized CODH at pH 7.2 and pH 10, CODH reduced with CO and then reoxidized in air at pH 7.2.** Spectra were obtained at 30 K using 514.5 nm excitation. Resonance Raman spectra of FAD, desulfo-xanthine oxidase, and plant sulfite oxidase, which is known to possess a $MoO_2$ core [26], are shown in the *upper panel* for comparison.

loss of proton splitting even as weak as 3 G would have led to a demonstrable narrowing of the features upon substitution into $D_2O$. We conclude that the EPR-active Mo(V) state has no equatorial Mo-OH, and that the equatorial position is occupied by a fully deprotonated Mo=O group. This being the case, it is very unlikely that there will be one in the more oxidized Mo(VI) state of the oxidized enzyme. The equatorial oxygen ligand of Mo in oxidized CODH has been assigned as either a Mo-OH group on the basis of the high resolution crystal structure (7) or a second Mo=O from x-ray absorption studies (15). Our EPR result is consistent with the XAS work indicating a $MoO_2$ core in the active site of oxidized enzyme.

In a final EPR experiment, the spectrum of CODH reduced with ^{13}C-labeled CO (Fig. 7E) was found to exhibit significant line-broadening, even (weak) doublet structure ~3425 and 3470 G. The splitting of Mo(V) signal by ^{13}C-labeled CO clearly demonstrates that $CO/CO_2$ is present in the signal-giving species of substrate-reduced enzyme.

The resonance Raman (rR) spectra of oxidized CODH at pH 7 and 10 (Fig. 8) exhibit features attributable to FAD (1300–1400 cm$^{-1}$), Fe/S (300–350 cm$^{-1}$), and two distinct bands at 895 and 861 cm$^{-1}$, which we ascribe to the symmetric ($\nu_s$) and antisymmetric ($\nu_{as}$) Mo-O$_{oxo}$ stretching modes, respectively, arising from a $MoO_2$ core. These vibrational frequencies are similar to those previously observed in sulfite oxidase: $\nu_s$(Mo-O$_{oxo}$) = 896 cm$^{-1}$ and $\nu_{as}$ (Mo=O) = 864 cm$^{-1}$ (35, 36), and in Mo(VI) model compounds: $\nu_s$(Mo-O$_{oxo}$) from 858 to 938 cm$^{-1}$, and $\nu_{as}$(Mo-O$_{oxo}$) from 835 to 898 cm$^{-1}$ (37). The present rR results are thus also consistent with a $CuSMoO_2$ core in the oxidized enzyme (15).

A CODH sample reduced with CO and then reoxidized in air reveals an rR spectrum similar to that of desulfo-XO (Fig. 8, *upper panel*), indicating that handling of the protein in this way results in loss of the Mo-S-Cu bond, yielding a catalytically inactive $MoO_3$ core. This result is consistent with the previously observed inactivation of CODH in the presence of both CO and $O_2$ (4).

## CONCLUSIONS

In the present work, we have examined the oxidation of CO by CODH using kinetic and spectroscopic methods. The enzyme exhibits a steady-state $k_{cat}$ of 93.3 s$^{-1}$, similar to previous work (7). On the other hand, the observed rate constant $k_{red}$ for the reductive-half reaction of CODH with CO is 51.1 s$^{-1}$ at 25 °C and pH 7.2, reflecting an intrinsic $k_{red}$ of 102 s$^{-1}$ that is in good agreement with the steady-state $k_{cat}$ of 93.3 s$^{-1}$. The absence of any dependence of $k_{red}$ on [CO] is consistent with

the spectrum, and are readily reproduced in simulations (Fig. 7F, *dashed line*). The parameters from this simulation are $g_{1,2,3}$ = 2.0010, 1.9604, 1.9549 and $A_{1,2,3}$ = 117, 164, 132 MHz, with Euler angles $\alpha = 0$, $\beta = 40$, $\gamma = 40$. The high quality of the simulation demonstrates that the EPR signal in question arises from a single paramagnetic species.

CODH reduced with CO in $D_2O$ shows the identical EPR spectrum (Fig. 7D) as in $H_2O$, with no discernible narrowing even of the observed linewidths. The expected hyperfine splitting for an equatorial Mo-OH in systems analogous to that seen in CO dehydrogenase (that is, those having a square pyramidal coordination geometry for the molybdenum with an apical Mo=O group) is in the range 3–14 G, and splittings of this magnitude yield demonstrable doublet structure in the EPR signal. In the "Rapid type 1" signal of xanthine oxidase, for example, a doublet of doublets is observed due to proton hyperfine splitting from the equatorial Mo-OH and Mo-SH ligands of 3 and 14 G, respectively. In the "Rapid type 2" signal of this enzyme, the Mo-OH splitting grows to 13 G, yielding a 1:2:1 triplet due to two approximately equally strongly coupled protons. As demonstrated in the classic work of Bray and coworkers (33, 34), the Mo-OH and Mo-SH protons of the "rapid" signals of xanthine oxidase are solvent-exchangeable, and substitution into $D_2O$ collapses the hyperfine structure to give a single line for each principal g-value of the signals.[3] The complexity of the EPR signal seen here with CO dehydrogenase notwithstanding, its linewidths (5–6 G) are comparable to those seen for the signals observed with xanthine oxidase and

---

[3] Substitution of the $^2$H nucleus (I = 1) for the $^1$H (I = $^1/_2$) results in loss of observable hyperfine structure because the nuclear moment of $^2$H is less than 1/3 that of $^1$H, with the result that the 1:1:1 triplet expected *a priori* is not resolved.

the rapid formation of a complex of CO with enzyme prior to substrate oxidation. Previous computational and model compound studies have in fact suggested that the first step of the catalytic cycle is CO binding to the Cu(I) of the active site (17, 18). The good agreement between steady-state and reductive half-reaction kinetics, as well as their similar pH dependences suggest that the reductive-half reaction is the rate-limiting step in CODH catalysis.

Significant FADH$^{\bullet}$ accumulation is seen in the course of reductive titrations of CODH with sodium dithionite, with ~20% of FADH$^{\bullet}$ accumulating at maximum on the basis of EPR integration. Transient accumulation of FADH$^{\bullet}$, as manifested in an absorption increase above 550 nm, is also observed in the course of the reaction of CODH with CO at pH 7.2 and below. The results indicate that the FAD of CODH has a significantly higher reduction potential (~30 mV) relative to the [2Fe-2S] clusters of the enzyme than is seen in XOR.

Our results indicate that the EPR signal shown in Fig. 7, *B–F* arises from a single Mo(V) species ($g_{1,2,3}$ = 2.0010, 1.9604, 1.9549) exhibiting strong coupling to copper ($A_{1,2,3}$ = 117, 164, 132 MHz), as well as weaker coupling to the carbon of CO. No proton coupling is evident, as reflected in the absence of any effect when the sample is prepared in D$_2$O, indicating that neither the paramagnetic Mo(V) species nor the Mo(VI) state of oxidized enzyme is likely to possess a protonated Mo-OH group. The molybdenum is thus best formulated as having a MoO$_2$ core rather than MoO(OH), a conclusion consistent with our resonance Raman results, with bands evident at 895 and 861 cm$^{-1}$ that are assigned to symmetric and antisymmetric MoO$_2$ stretching modes, respectively. This interpretation is consistent with previous x-ray absorption spectroscopic results with CODH (15).

## REFERENCES

1. Meyer, O., and Schlegel, H. G. (1978) *Arch. Microbiol.* **118,** 35–43
2. Meyer, O., and Schlegel, H. G. (1980) *J. Bacteriol.* **141,** 74–80
3. Cypionka, H., and Meyer, O. (1983) *J. Bacteriol.* **156,** 1178–1187
4. Meyer, O., Gremer, L., Ferner, R., Ferner, M., Dobbek, H., Gnida, M., Meyer-Klaucke, W., and Huber, R. (2000) *Biol. Chem.* **381,** 865–876
5. Ragsdale, S. W., and Kumar, M. (1996) *Chem. Rev.* **96,** 2515–2540
6. Dobbek, H., Gremer, L., Meyer, O., and Huber, R. (1999) *Proc. Natl. Acad. Sci. U.S.A.* **96,** 8884–8889
7. Dobbek, H., Gremer, L., Kiefersauer, R., Huber, R., and Meyer, O. (2002) *Proc. Natl. Acad. Sci. U.S.A.* **99,** 15971–15976
8. Hänzelmann, P., Dobbek, H., Gremer, L., Huber, R., and Meyer, O. (2000) *J. Mol. Biol.* **301,** 1221–1235
9. Gremer, L., Kellner, S., Dobbek, H., Huber, R., and Meyer, O. (2000) *J. Biol. Chem.* **275,** 1864–1872
10. Kang, B. S., and Kim, Y. M. (1999) *J. Bacteriol.* **181,** 5581–5590
11. Schübel, U., Kraut, M., Mörsdorf, G., and Meyer, O. (1995) *J. Bacteriol.* **177,** 2197–2203
12. Santiago, B., Schübel, U., Egelseer, C., and Meyer, O. (1999) *Gene* **236,** 115–124
13. Hille, R. (1996) *Chem. Rev.* **96,** 2757–2816
14. Moersdorf, G., Frunzke, K., Gadkari, D., and Meyer, O. (1992) *Biodegradation* **3,** 61–82
15. Gnida, M., Ferner, R., Gremer, L., Meyer, O., and Meyer-Klaucke, W. (2003) *Biochemistry* **42,** 222–230
16. Hofmann, M., Kassube, J. K., and Graf, T. (2005) *J. Biol. Inorg. Chem.* **10,** 490–495
17. Siegbahn, P. E., and Shestakov, A. F. (2005) *J. Comput. Chem.* **26,** 888–898
18. Gourlay, C., Nielsen, D. J., White, J. M., Knottenbelt, S. Z., Kirk, M. L., and Young, C. G. (2006) *J. Am. Chem. Soc.* **128,** 2164–2165
19. Hänzelmann, P., and Meyer, O. (1998) *Eur. J. Biochem.* **255,** 755–765
20. Bradford, M. M. (1976) *Anal. Biochem.* **72,** 248–254
21. Meyer, O., and Rajagopalan, K. V. (1984) *J. Biol. Chem.* **259,** 5612–5617
22. Resch, M., Dobbek, H., and Meyer, O. (2005) *J. Biol. Inorg. Chem.* **10,** 518–528
23. Kraut, M., Hugendieck, I., Herwig, S., and Meyer, O. (1989) *Arch. Microbiol.* **152,** 335–341
24. Di Lorio (1981) *Methods Enzymol.* **76,** 58
25. Dean, J. A. (1972) *Lange's Handbook of Chemistry,* 12$^{th}$ Ed., McGraw-Hill, New York
26. Olson, J. S., Ballou, D. P., Palmer, G., and Massey, V. (1974) *J. Biol. Chem.* **249,** 4363–4382
27. Hille, R. (1991) *Biochemistry* **30,** 8522–8529
28. Deleted in proof
29. McWhirter, R. B., and Hille, R. (1991) *J. Biol. Chem.* **266,** 23724–23731
30. Kim, J. H., Ryan, M. G., Knaut, H., and Hille, R. (1996) *J. Biol. Chem.* **271,** 6771–6780
31. Leimkühler, S., Stoker, A. L., Igarashi, K., Nishino, T., and Hille, R. (2004) *J. Biol. Chem.* **279,** 40437–40444
32. Bray, R. C., George, G. N., Lange, R., and Meyer, O. (1983) *Biochem. J.* **211,** 687–694
33. Pick, F. M., and Bray, R. C. (1969) *Biochem. J.* **114,** 735–742
34. Bray, R. C., Barber, M. J., and Lowe, D. J. (1978) *Biochem. J.* **171,** 653–658
35. Hemann, C., Hood, B. L., Fulton, M., Hänsch, R., Schwarz, G., Mendel, R. R., Kirk, M. L., and Hille, R. (2005) *J. Am. Chem. Soc.* **127,** 16567–16577
36. Garton, S. D., Garrett, R. M., Rajagopalan, K. V., and Johnson, M. K. (1997) *J. Am. Chem. Soc.* **119,** 2590–2591
37. Johnson, M. K. (2004) in *Diothiolene Chemistry: Progress in Inorganic Chemistry* (Stiefel, E. I., ed) Vol. 52, pp. 213–266, John Wiley & Sons, Inc., Hoboken, NJ